From fractional Chern insulators to Abelian and non-Abelian fractional quantum Hall states: Adiabatic continuity and orbital entanglement spectrum

Zhao Liu[1,2,*] and Emil J. Bergholtz[3,†]

[1]*Beijing Computational Science Research Center, Beijing, 100084, China*

[2]*Institute of Physics, Chinese Academy of Sciences, Beijing, 100190, China*

[3]*Dahlem Center for Complex Quantum Systems and Institut für Theoretische Physik, Freie Universität Berlin, Arnimallee 14, 14195 Berlin, Germany*

(Received 25 September 2012; published 14 January 2013)

The possibility of realizing lattice analogs of fractional quantum Hall (FQH) states, so-called fractional Chern insulators (FCIs), in nearly flat topological (Chern) bands has attracted a lot of recent interest. Here, we make the connection between Abelian as well as non-Abelian FQH states and FCIs more precise. Using a gauge-fixed version of Qi's Wannier basis representation of a Chern band, we demonstrate that the interpolation between several FCI states, obtained by short-range lattice interactions in a spin-orbit-coupled kagome lattice model, and the corresponding continuum FQH states is smooth: the gap remains approximately constant and extrapolates to a finite value in the thermodynamic limit, while the low-lying part of the orbital entanglement spectrum remains qualitatively unaltered. The orbital entanglement spectra also provide a first glimpse of the edge physics of FCIs via the bulk-boundary correspondence. Corroborating these results, we find that the squared overlaps between the FCI and FQH ground states are as large as 98.7% for the 8-electron Laughlin state at $\nu = \frac{1}{3}$ (consistent with an earlier study) and 97.8% for the 10-electron Moore-Read state at $\nu = \frac{1}{2}$. For the bosonic analogs of these states, the adiabatic continuity is also shown to hold, albeit with somewhat smaller associated overlaps, etc. Although going between the Chern bands to the Landau-level problem is often smooth, we show that this is not always the case by considering fermions at filling fraction $\nu = \frac{4}{5}$, where the interpolation between Hamiltonians describing the two systems results in a phase transition.

DOI: 10.1103/PhysRevB.87.035306 PACS number(s): 73.43.Cd, 71.10.Fd, 73.21.Ac

I. INTRODUCTION

After Haldane's seminal work modeling an integer quantum Hall (IQH) effect in a simple lattice model,[1] it took over 20 years until it was recently realized that similar ideas were used to emulate lattice analogs of fractional quantum Hall (FQH) states.[2–6] These states, termed fractional Chern insulators (FCIs), have a number of appealing traits: most saliently they do not require an external magnetic field and they might, in principle, persist at elevated temperatures.

While the basic ingredient needed for the IQH effect is a band with nonzero Chern number (and a finite band gap), an additional prerequisite for the FCIs is that these bands are only weakly dispersive, thus enhancing the effect of interactions within the band. Following the initial suggestions,[2–4] there are by now many known models with nearly flat bands carrying nonzero Chern number, including intriguing solid-state proposals[2,7–12] and possible cold-atom realizations.[13] Although there is plenty of numerical evidence for FCI analogs of Laughlin states,[4–6] hierarchy/composite fermion states,[14–16] as well as non-Abelian states,[17–19] the physics in Chern bands is only identical to that of a Landau level in a very idealized limit.[17,20] In actual lattice models, however, the distinctions are rather striking such as particle-hole symmetry breaking[15,16] and the emergence of qualitatively new competing compressible states,[15] underscoring the need for a better understanding of theses systems at a quantitative level.

In an insightful paper, Qi introduced a Wannier basis representation of a Chern band mincing the Landau gauge wave functions in the continuum, and thereby paved the way towards a more direct comparison between FCI and FQH states.[21] Indeed, Scaffidi and Möller recently used this mapping to convincingly show that the $\nu = \frac{1}{2}$ bosonic FCI state on the honeycomb lattice is indeed smoothly connected to the Laughlin state describing the continuum FQH state at the same filling fraction.[22] However, a direct implementation of Qi's Wannier mapping is not always successful, e.g., wave-function overlaps with FQH model states often turn out to be minuscule even in models where there are well-established FCI phases, due to the finite-size properties (nonorthogonality) of the Wannier functions and, in principle, also because the two systems carry independent gauge degrees of freedom. This issue was considered in detail by Wu *et al.* who also came up with an involved, yet elegant, prescription that remedies these problems and showed that it leads to impressive overlaps between the fermionic FCI at $\nu = \frac{1}{3}$ and the corresponding Laughlin FQH state.[23]

In this work, we apply the Wannier state mapping[21] adopted to finite-size systems[23] to both Abelian and non-Abelian FCI phases. We demonstrate the adiabatic continuity between these states and their corresponding FQH analogs (Laughlin[24] and Moore-Read[25] states) by showing that the gap remains essentially unaltered when interpolating between the FCI and FQH Hamiltonians as well as studying the overlaps with the model FQH states which turn out to remain high throughout the interpolation. Moreover, we report on the first studies of orbital entanglement spectra[26] (OES) of the FCI states. In contrast to the earlier particle entanglement spectrum[27] (PES) studies[6] which probe the quasihole physics, our OES studies, based on a cut in (Wannier) orbital space,[28] provide a test of the edge physics in FCI phases. The upshot of these studies is that the FCI states considered here are, in a well-defined sense, closer to the idealized model FQH wave functions than

FQH states obtained for more realistic (Coulomb) interactions in continuum Landau level. Underscoring that these results are indeed nontrivial, we also provide an example where the interpolation between the Landau-level physics and the interacting Chern band problem is not smooth by considering fermions at $\nu = \frac{4}{5}$.

The remainder of this work is organized as follows. In Sec. II, we give a relatively detailed description of the Wannier mapping providing a bridge between the description of Chern bands and continuum Landau levels on a torus. Section III contains our main results on the adiabatic continuity and the OES studies focusing on electronic (fermionic) states (corresponding results for bosons are contained in the Appendixes). Finally, we discuss our findings in Sec. IV.

II. MODEL AND METHODS

In this section, we put the description of fractional quantum Hall systems in the continuum and fractional Chern insulators in the lattice on the same footing. First, we discuss the lowest Landau level (LLL) on a torus,[29] and then we go on to discuss a suitably adapted version of the Wannier function mapping of Chern bands in a finite-size system.[23] This provides the necessary framework for a direct quantitative comparison between FCIs with FQH states despite the fact that the two systems have different symmetries. Finally, we give a specific kagome lattice model that we use throughout this work to study the FQH-FCI correspondence.

A. Quantum Hall states

We consider N particles projected to the lowest Landau level on a twisted torus spanned by two basic vectors $\mathbf{L}_1 = L_1\mathbf{v}_1(\alpha)$ and $\mathbf{L}_2 = L_2\mathbf{v}_2$, where $\mathbf{v}_1(\alpha) = \sin\alpha\mathbf{e}_x + \cos\alpha\mathbf{e}_y$, $\mathbf{v}_2 = \mathbf{e}_y$, where α is the twisted angle of the torus, and $L_{1(2)}$ is the length of the basic vector (in units of the magnetic length). Assuming the number of flux quanta N_s through the surface of the torus is an integer, the magnetic translation invariance in the $\mathbf{v}_1$ and $\mathbf{v}_2$ directions leads to $L_1L_2\sin\alpha = 2\pi N_s$. There are precisely N_s single-particle states $|\psi_j\rangle$ in the lowest Landau level that we choose as maximally to be localized in the $\mathbf{e}_x$ direction (but delocalized in the $\mathbf{e}_y$ direction) as

$$\langle x,y|\psi_j\rangle = \left(\frac{1}{\sqrt{\pi}L_2}\right)^{\frac{1}{2}}\sum_{n=-\infty}^{+\infty}\exp\left\{\mathrm{i}\left(\frac{2\pi j}{L_2}+nL_1\sin\alpha\right)\times\left(y-\frac{2\pi j}{L_2}\cot\alpha-nL_1\cos\alpha\right)-\frac{1}{2}\left(x-\frac{2\pi j}{L_2}-nL_1\sin\alpha\right)^2\right\}, \quad (1)$$

where $j = 0,1,2,\ldots,N_s-1$ is the single-particle momentum in units of $2\pi/L_2$. Note that ψ_j is quasiperiodic and centered along the line $x = 2\pi j/N_2$. We define N_0 as the greatest common divisor of N and N_s, namely, $N_0 \equiv \mathrm{GCD}(N,N_s)$. Then, $p \equiv N/N_0$ and $q \equiv N_s/N_0$ are coprime. There are two translation operators T_α ($\alpha = 1,2$) that commute with the many-body Hamiltonian (as with any translational invariant operator) and obey $T_1T_2 = e^{2\pi\mathrm{i}p/q}T_2T_1$. T_1 corresponds to an $\mathbf{e}_y$ translation and T_2 translates a many-body state one lattice constant $2\pi/L_2$ in the $\mathbf{e}_x$ direction. At filling factor $\nu = p/q$, because T_2^q commutes with T_1, we can diagonalize certain many-body Hamiltonian H_{FQH} in the LLL orbital basis and obtain the many-body ground states $|\Psi_{\mathrm{FQH}}(K_1,K_2)\rangle$ as the common eigenstates of T_1 and T_2^q with eigenvalues $e^{2\pi\mathrm{i}K_1/N_s}$ and $e^{2\pi\mathrm{i}K_2/N_0}$, where K_1 can be regarded as the total momentum in the $\mathbf{e}_x$ direction. It directly follows that the degeneracy of $|\Psi_{\mathrm{FQH}}(K_1,K_2)\rangle$ is at least q-fold, among which we can always pick up q-fold center-of-mass degenerate states with different K_1 that are connected by the operator T_2^k ($k = 0,1,\ldots,q-1$).

For later convenience, we also introduce an alternative description of the translational symmetry on the torus. Suppose N_s has two factors N_1 and N_2, namely, $N_s = N_1 \times N_2$. After defining $N_{0,1} \equiv \mathrm{GCD}(N,N_1)$ and $q_1 \equiv N_1/N_{0,1}$, we can introduce two translation operators $S_1 = (T_2)^{q/q_1}$ and $R_2 = T_1^{q_1}$. Because S_1 commutes with R_2, we can make the many-body ground states as their common eigenstates. Within this description of the translational symmetry, the q-fold center-of-mass degenerate states are

$$|\Psi_{\mathrm{FQH}}(s,r)\rangle = \frac{1}{\sqrt{q_1}}\sum_{m=0}^{q_1-1}e^{2\pi\mathrm{i}m\left(\frac{sN-K_2}{N_0q_1}\right)}S_1^mT_2^r|\Psi_{\mathrm{FQH}}(K_1,K_2)\rangle, \quad (2)$$

where $s = 0,1,\ldots,q_1-1$, $r = 0,1,\ldots,q/q_1-1$. If we choose N_1 and N_2 appropriately, we can make $q_1 = 1$. Then, $|\Psi_{\mathrm{FQH}}(s,r)\rangle$ and $|\Psi_{\mathrm{FQH}}(K_1,K_2)\rangle$ reduce to the same description.

B. Chern insulators

Now, we move our attention from FQH states in the continuum to the FCIs in the lattice. We consider a two-dimensional (2D) lattice on the torus with two lattice vectors $\mathbf{v}_1(\beta) = \sin\beta\mathbf{e}_x + \cos\beta\mathbf{e}_y$ and $\mathbf{v}_2 = \mathbf{e}_y$. The number of unit cells is N_1 and N_2 in respective direction and there are s sites in each unit cell. The states in the first Brillouin zone (1BZ) can be labeled by a 2D momentum $\mathbf{k} = (k_1,k_2)$ where $k_i = 0,1,\ldots,N_i-1$. In momentum space, the single-particle Hamiltonian can be written as $H = \sum_{\mathbf{k}\in\mathrm{BZ}}(c^\dagger_{\mathbf{k},1},\ldots,c^\dagger_{\mathbf{k},s})h(\mathbf{k})(c_{\mathbf{k},1},\ldots,c_{\mathbf{k},s})^T$ and a band structure is formed. We focus on a single, isolated band $|\mathbf{k}\rangle = \sum_{\alpha=1}^s u_\alpha(\mathbf{k})c^\dagger_{\mathbf{k},\alpha}|\mathrm{vac}\rangle$, where $u_\alpha(\mathbf{k})$ is the corresponding eigenfunction of $h(\mathbf{k})$, and suppose N interacting particles fractionally fill in this band. If the interaction Hamiltonian H_{FCI} is chosen appropriately, the ground states of this interacting many-body system are FCI states $|\Psi_{\mathrm{FCI}}\rangle$ at certain filling factors $\nu = N/(N_1N_2)$.

To compare the FCI states with the theoretically much better understood FQH states, we need to expand $|\Psi_{\mathrm{FCI}}\rangle$ in a basis with single-particle states that mimic the LLL states [Eq. (1)]. An appropriate choice is the Wannier basis, the single-particle state $|X,k_2\rangle$ of which is localized in the $\mathbf{v}_1$ direction but delocalized in the $\mathbf{v}_2$ direction, where X is the position in the $\mathbf{v}_1$ direction and k_2 is the momentum (in units of $2\pi/N_2$) in the $\mathbf{v}_2$ direction.[21,23]

In a $N_1 \times N_2$ finite-size lattice, when focusing on one fractionally filled band with Chern number $\mathcal{C}$, the (lattice version of the) Berry connection in the $\mathbf{v}_1$ direction can be defined as $\mathcal{A}_1(k_1,k_2) = \sum_\alpha e^{-\mathrm{i}2\pi\epsilon^1_\alpha/N_1}u^*_\alpha(k_1,k_2)u_\alpha(k_1+1,k_2)$, where ϵ^1_α is the $\mathbf{v}_1$-direction relative displacement of site α in a

unit cell. Similarly, we can define the Berry connection in the $\mathbf{v}_2$ direction as $\mathcal{A}_2(k_1,k_2) = \sum_\alpha e^{-\mathrm{i}2\pi\epsilon_\alpha^2/N_2} u_\alpha^*(k_1,k_2)u_\alpha(k_1,k_2+1)$. To restore the orthogonality between different Wannier functions, we need to introduce unitary Berry connections[23] $A_{1(2)}(k_1,k_2) = \mathcal{A}_{1(2)}(k_1,k_2)/|\mathcal{A}_{1(2)}(k_1,k_2)|$. Then, the unitary Wilson loops are $W_1(k_2) = \prod_{k_1=0}^{N_1-1} A_1(k_1,k_2)$ and $W_2(k_1) = \prod_{k_2=0}^{N_2-1} A_2(k_1,k_2)$, whose argument angles are picked in $(-2\pi,0]$. After defining a shift δ_2 as the cardinality of the set $\{k_2 = 0,1,\ldots,N_2-1 | \arg[W_1(k_2)] > \arg[W_1(0)]\}$, we can introduce a principal Brillouin zone (pBZ) as the set of k_2 satisfying $\mathcal{C}k_2 + \delta_2 \in [0,N_2)$ and move k_2 from 1BZ to pBZ.

After introducing $[\lambda_1(k_2)]^{N_1} \equiv W_1(k_2)$ and $[\lambda_2(k_1)]^{N_2} \equiv W_2(k_1)$, where we choose the argument angle $\arg[\lambda_1(k_2)] \in (-2\pi/N_1,0]$ and $\arg[\lambda_2(k_1)] \in (-2\pi/N_2,0]$, we can define the Wannier function localized in the $\mathbf{v}_1$ direction as

$$|X,k_2\rangle = \frac{e^{\mathrm{i}\Phi(k_2)}}{\sqrt{N_1}} \sum_{k_1=0}^{N_1-1} e^{-\mathrm{i}\frac{2\pi k_1}{N_1}X} \left\{ \frac{[\lambda_1(k_2)]^{k_1}}{\prod_{\kappa=0}^{k_1-1} A_1(\kappa,k_2)} \right\} |k_1,k_2\rangle,$$

where k_2 is in pBZ and $\Phi(k_2)$ is independent of X and needs to be fixed by a special prescription (see Appendix C for details). Letting $j^{X,k_2} = N_2X + \mathcal{C}k_2 + \delta_2$, we can build a one-to-one map between $|X,k_2\rangle$ and $|\psi_j\rangle$.

Considering the one-to-one map between the Wannier orbital and the LLL orbital as well as their similar localizing properties, the FCI states $|\Psi_{\mathrm{FCI}}\rangle$ in the Wannier basis will be very well approximated by the lattice version of FQH states constructed as[30]

$$\left|\Psi_{\mathrm{FQH}}^{\mathrm{lat}}(s,r)\right\rangle = \sum_{\{X,k_2\}} |\{X,k_2\}\rangle\langle\{j^{X,k_2}\}|\Psi_{\mathrm{FQH}}(s,r)\rangle, \qquad (3)$$

where $|\{\ldots\}\rangle$ is the many-body occupation configuration over the single-particle state $|\ldots\rangle$ [one can find that $|\Psi_{\mathrm{FQH}}(s,r)\rangle$ in the LLL orbital basis and its lattice version $|\Psi_{\mathrm{FQH}}^{\mathrm{lat}}(s,r)\rangle$ in the Wannier basis have a common description]. However, it is important to note that $|\Psi_{\mathrm{FQH}}^{\mathrm{lat}}(s,r)\rangle$ will in general differ from $|\Psi_{\mathrm{FCI}}\rangle$ since the Hamiltonians of the two systems have vastly different origins. Moreover, as discussed in the following, the symmetries of the two models are different.

C. Symmetries

The FQH Hamiltonian in the LLL on the torus conserves center-of-mass position corresponding to momentum $K_1 = \sum_{i=1}^{N} j_i \pmod{N_s}$. However, the corresponding quantity is not conserved for the FCI problem despite the fact that there is a one-to-one correspondence $j^{X,k_2} = N_2X + \mathcal{C}k_2 + \delta_2$ between $|X,k_2\rangle$ and $|\psi_j\rangle$ which allows us to calculate a total 1D momentum $\sum_{i=1}^{N}(j^{X,k_2})_i \pmod{N_1N_2}$. Instead, the translational symmetry (in real space) in the directions of the two lattice vectors in the Chern band implies a conserved two-dimensional momentum, which leads to a reduced symmetry for the FCI Hamiltonian in the Wannier basis: only $J_1 = \sum_{i=1}^{N}(j^{X,k_2})_i \pmod{N_2}$ is conserved. (Another manifestation of the lower symmetry in the FCI problem is reflected in the lack of particle-hole symmetry.[15])

The symmetry difference is indeed a generic effect due to the underlying lattice where the Berry curvature necessarily varies in reciprocal space as long as the number of bands is finite. In an ideal limit, however, the FCI Hamiltonian will have the same emergent symmetries as the FQH Hamiltonian.[20]

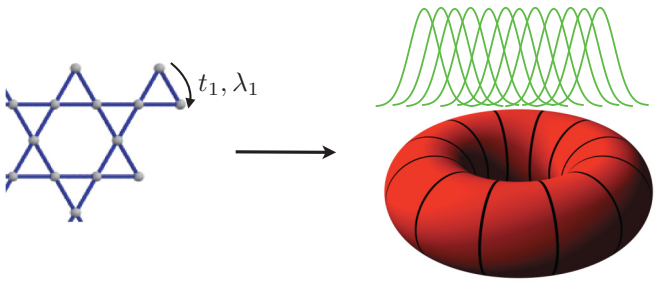

FIG. 1. (Color online) Schematic picture of the mapping of a flat Chern band in the lattice model to a continuum Landau level in terms of Wannier states.

D. Kagome lattice model

In the following, we focus on a special lattice model, namely, the kagome lattice model proposed in Ref. 2, to investigate the FCI-FQH correspondence. The single-particle Hamiltonian of the kagome lattice model (cf. Fig. 1) in the real space is

$$H = t_1 \sum_{\langle i,j\rangle,\sigma} c_{i\sigma}^\dagger c_{j\sigma} + \mathrm{i}\lambda_1 \sum_{\langle i,j\rangle,\alpha,\beta} (\hat{\mathbf{E}}_{ij} \times \hat{\mathbf{R}}_{ij}) \cdot \sigma_{\alpha\beta} c_{i\alpha}^\dagger c_{j\beta},$$

where $\hat{\mathbf{E}}_{ij}$ is the normalized $|\hat{\mathbf{E}}_{ij}| = 1$ electric field arising from an ion at the center of each hexagon as experienced by a particle hopping along the unit vector $\hat{\mathbf{R}}_{ij}$ from site i to site j. In this work, we consider electrons are spin-polarized (all spin up) particles and set $t_1 = -1$ while using band structures corresponding to various λ_1 as input to our studies of interactions projected to nontrivial bands. In the momentum space, we have three energy bands, the lowest one of which has Chern number $\mathcal{C} = 1$. As customary,[6] we take the flat band limit and project the interaction Hamiltonian H_{FCI} to this $\mathcal{C} = 1$ band. Recent numerical work has indeed shown that both Abelian and non-Abelian FCI states exist in this model.[19]

III. CONTINUITY BETWEEN FQH AND FCI

As discussed above, the FQH Hamiltonian and FCI Hamiltonian have different symmetries. However, they have a similar expression written in second-quantized form. Taking two-body interactions as an example, we have $H_{\mathrm{FQH}} = \sum_{j_1j_2j_3j_4=0}^{N_s-1} \delta_{j_1+j_2,j_3+j_4}^{\mathrm{mod}N_s} V_{j_1j_2j_3j_4}^{\mathrm{FQH}} c_{j_1}^\dagger c_{j_2}^\dagger c_{j_3} c_{j_4}$ for the FQH case, where $c_j^\dagger$ (c_j) creates (annihilates) a particle in the state $|\psi_j\rangle$, while we have $H_{\mathrm{FCI}} = \sum_{j_1j_2j_3j_4=0}^{N_1N_2-1} \delta_{j_1+j_2,j_3+j_4}^{\mathrm{mod}N_2} V_{j_1j_2j_3j_4}^{\mathrm{FCI}} c_{j_1}^\dagger c_{j_2}^\dagger c_{j_3} c_{j_4}$, where $c_j^\dagger$ (c_j) creates (annihilates) a particle in the state $|X,k_2\rangle$ with $j = XN_2 + \mathcal{C}k_2 + \delta_2$ for the FCI case. Therefore, the structure of the Hilbert space of FCIs in the Wannier basis is the same as that of FQH systems in the LLL orbital basis if we set $N_s = N_1 \times N_2$. This makes it meaningful to consider an interpolating Hamiltonian as follows:

$$H(\lambda) = \lambda w_{\mathrm{FCI}} H_{\mathrm{FCI}} + (1-\lambda) w_{\mathrm{FQH}} H_{\mathrm{FQH}}, \qquad (4)$$

where $\lambda \in [0,1]$ is the interpolation parameter and w_{FCI} and w_{FQH} are the energy rescaling factors that can make the

energy gap at $\lambda = 0$ and 1 equal to 1 (in the cases where we find adiabatic continuity below it is well established that the gap survives in the thermodynamic limit at $\lambda = 0$ and 1, respectively). We then diagonalize Eq. (4) in each $J_1 = 0,1,\ldots,N_2 - 1$ sector and analyze the energy gap and the ground states as a function of λ, in order to examine whether the FCI states are adiabatically connected to the corresponding FQH model states.

A. Fermions at $\nu = \frac{1}{3}$

We start our discussion by focusing on the fermions at filling factor $\nu = \frac{1}{3}$. On the FQH side, we choose the Hamiltonian as $H_{\rm FQH} = \sum_{i<j} \nabla_i^2 \delta^2(\mathbf{r}_i - \mathbf{r}_j)$. Then, the ground states are exact threefold-degenerate fermionic Laughlin states with zero energy. On the FCI side, the Hamiltonian is set as the nearest-neighbor interaction $H_{\rm FCI} = \sum_{\langle ij \rangle} n_i n_j$. The ground states are three nearly degenerate states separated by a gap from the excited states. Since $\beta = \pi/3$ for the kagome lattice, we set $\alpha = \pi/3$ also for the twisted Landau-level torus. This choice is further justified by the large overlap between the FCI states at $\lambda = 1$ and the Laughlin states at $\lambda = 0$ (see the following discussion).

We find that for each $\lambda \in [0,1]$, there are three nearly degenerate states separated by a sizable gap Δ from excited levels in the energy spectrum. We report the evolution of Δ with λ for various system sizes in Fig. 2(a). It can be seen that the gap never closes for any intermediate λ; in fact, it is always greater than one and has a maximal value at $\lambda \approx 0.4$–0.6. This

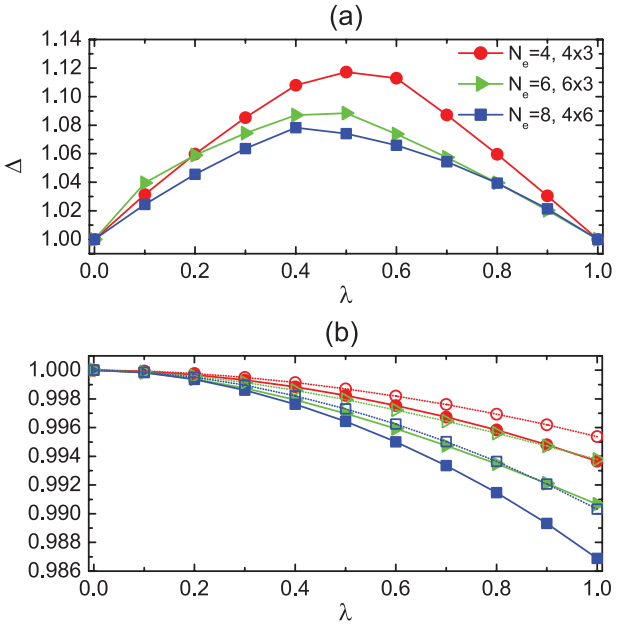

FIG. 2. (Color online) Results of the interpolation Eq. (4) for fermions at $\nu = \frac{1}{3}$ with $N_e = 4$ (red dot), $N_e = 6$ (green triangle), and $N_e = 8$ (blue square). In the FCI part, the lattice size is $N_1 \times N_2 = 4 \times 3$, $N_1 \times N_2 = 6 \times 3$, and $N_1 \times N_2 = 4 \times 6$, respectively; and $\lambda_1 = 1$. (a) The energy gap Δ does not close for any intermediate λ. (b) The total overlap $\mathcal{O}_{\rm tot}$ (filled symbol, solid line) and the average weight $\overline{\mathcal{W}}$ (empty symbol, dotted line) are still close to 1 at $\lambda = 1$. All of those demonstrate that the continuity holds for fermions at $\nu = \frac{1}{3}$.

provides strong evidence for the adiabatic continuity between FQH states and FCI states.

To further confirm that there is no phase transition between $\lambda = 0$ and 1, we study the properties of the ground manifold. We can define the total overlap as $\mathcal{O}_{\rm tot} = \frac{1}{d}\sum_{i=1}^{d}\sum_{j=1}^{d} |\langle \Psi^i_{\rm FQH}|\Psi^j(\lambda)\rangle|^2$, where d is the number of (nearly) degenerate states (here, $d = 3$), $|\Psi^j(\lambda)\rangle$ is the (nearly) degenerate state of $H(\lambda)$, and $|\Psi^j_{\rm FQH}\rangle = |\Psi^j(\lambda = 0)\rangle$ is the FQH state (here, the exact $\nu = \frac{1}{3}$ Laughlin state). We find that $\mathcal{O}_{\rm tot}$ decreases from 1 at $\lambda = 0$ smoothly to about 0.987 at $\lambda = 1$ for our largest system size $N_e = 8$ [Fig. 2(b)]. Therefore, the ground states do not change qualitatively during the interpolation from $\lambda = 0$ to 1, supporting that the FCI states are indeed very well captured by the lattice version of FQH states constructed by Eq. (3).

The entanglement spectrum[26] (ES) can usually provide us more insights than the overlap, which is only a single number and will necessarily vanish in the thermodynamic limit. For any bipartite pure state $|\Psi\rangle_{AB}$, it can be decomposed using the Schmidt decomposition

$$|\Psi\rangle_{AB} = \sum_i e^{-\xi_i/2} |\phi_i^A\rangle \otimes |\phi_i^B\rangle,$$

where the states $|\phi_i^A\rangle$ ($|\phi_i^B\rangle$) form an orthonormal basis for the subsystem A (B). $\{\xi_i \geqslant 0\}$ is defined as entanglement spectrum and is related to the eigenvalues η_i of the reduced density matrix $\rho_A = {\rm tr}_B(|\Psi\rangle_{AB\ AB}\langle\Psi|)$ of A as $\eta_i = e^{-\xi_i}$. In some previous works, the ES for particle cut has been investigated extensively to probe the quasihole excitation properties of FCI states. Here, we focus on another kind of ES, the OES for a cut in orbital space, to test the edge physics of FCI states.

We first briefly recall the OES of FQH states on the torus that has been studied in Refs. 31 and 32. The threefold-degenerate fermionic $\nu = \frac{1}{3}$ Laughlin states have the following simple representations in the orbital basis in the thin-torus limit[33] $L_2 = 0$ (for $N_e = 8$, $N_s = 24$):

$$\begin{aligned} &100100|\mathbf{100100100100}|100100,\\ &010010|\mathbf{010010010010}|010010,\\ &001001|\mathbf{001001001001}|001001. \end{aligned} \tag{5}$$

We bipartition the system into blocks A and B, which consist of l_A consecutive orbits and the remaining $N_s - l_A$ orbits, respectively [the bold block in Eq. (5) is our subsystem A]. After extracting the ES from the ground states, we label every ES level by the particle number $N_A = \sum_{j\in A} n_j$ and the total momentum $K_A = \sum_{j\in A} j n_j$ (mod N_s) in block A, where n_j is the particle number in the state $|\psi_j\rangle$. In this work, we concentrate on the case $l_A = N_s/2$.

In Refs. 31 and 32, it was shown that the resulting OES for the FQH state form towers that can be decomposed into the edge modes of the underlying conformal field theory (CFT). This combination comes about as the natural partition [Eq. (5)] gives a subsystem A with the geometry of a cylinder which has two edges on which gapless edge states with opposite chirality reside. An illuminating recent discussion of the connection between the OES, the CFT describing the edge, and matrix product states was given in Ref. 34.

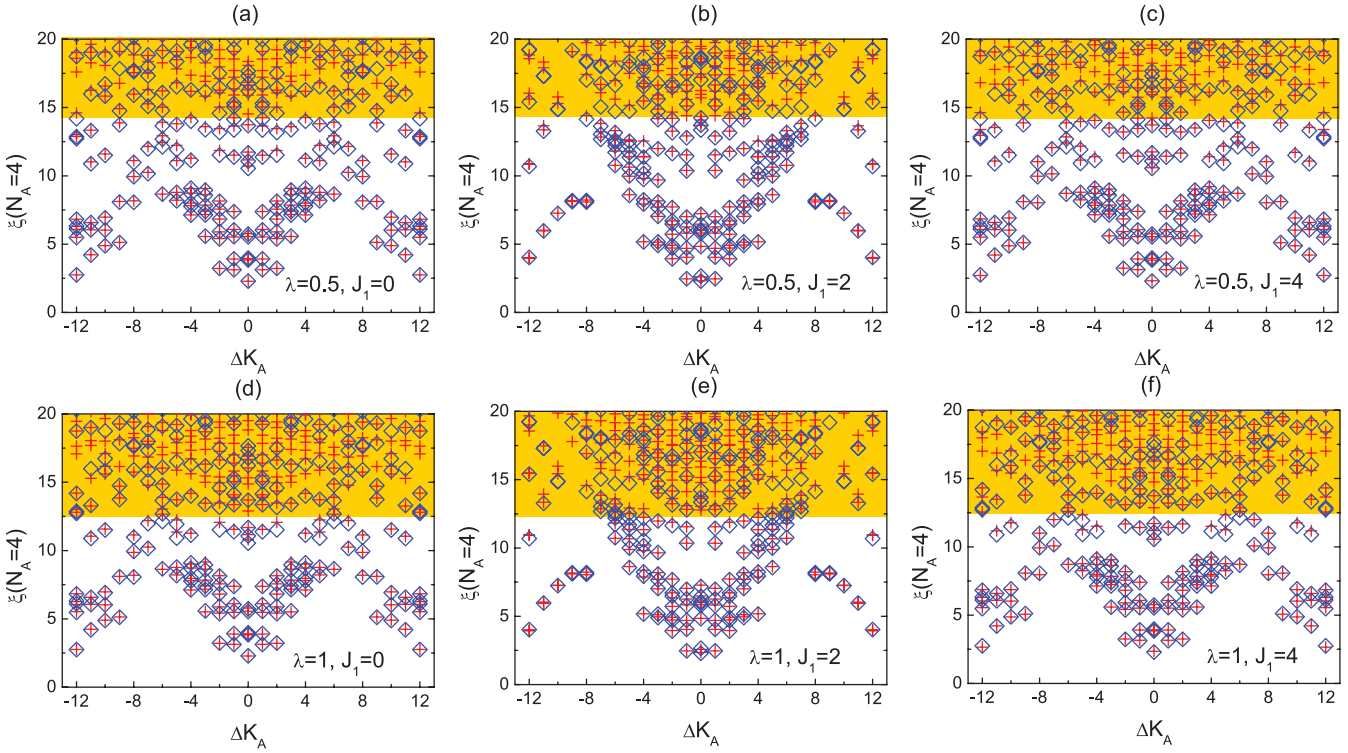

FIG. 3. (Color online) The orbital entanglement spectra (OES) of exact fermionic Laughlin states (blue diamond) and the projected nearly degenerate states $|\Psi_{\rm prj}^{J_1}(\lambda)\rangle$ (red cross) at $\nu=\frac{1}{3}$, $N_e=8$. The lattice size is $N_1\times N_2=4\times 6$ and $\lambda_1=1$ for the FCI part. In the left column, $J_1=0$, corresponding to the Laughlin state in the $K_1=12$ sector. In the middle column, $J_1=2$, corresponding to the Laughlin state in the $K_1=20$ sector. In the right column, $J_1=4$, corresponding to the Laughlin state in the $K_1=4$ sector. In (a), (b), and (c), $\lambda=0.5$. (a) The unprojected $|\Psi^{J_1=0}(\lambda)\rangle$ has weight $\mathcal{W}\approx 0.997\,30$ on the $K_1=12$ sector. The overlap with the Laughlin state $\mathcal{O}=|\langle\Psi_{\rm Lau}^{K_1=12}|\Psi^{J_1=0}(\lambda)\rangle|^2$ is 0.996 54. (b) The unprojected $|\Psi^{J_1=2}(\lambda)\rangle$ has weight $\mathcal{W}\approx 0.997\,32$ on the $K_1=20$ sector. The overlap with the Laughlin state $\mathcal{O}=|\langle\Psi_{\rm Lau}^{K_1=20}|\Psi^{J_1=2}(\lambda)\rangle|^2$ is 0.996 38. (c) The unprojected $|\Psi^{J_1=4}(\lambda)\rangle$ has weight $\mathcal{W}\approx 0.997\,32$ on the $K_1=4$ sector. The overlap $\mathcal{O}=|\langle\Psi_{\rm Lau}^{K_1=4}|\Psi^{J_1=4}(\lambda)\rangle|^2$ is 0.996 38. In (d), (e), and (f), $\lambda=1$. (d) The unprojected $|\Psi^{J_1=0}(\lambda)\rangle$ has weight $\mathcal{W}\approx 0.990\,62$ on the $K_1=12$ sector. The overlap with the Laughlin state $\mathcal{O}=|\langle\Psi_{\rm Lau}^{K_1=12}|\Psi^{J_1=0}(\lambda)\rangle|^2$ is 0.987 33. (e) The unprojected $|\Psi^{J_1=2}(\lambda)\rangle$ has weight $\mathcal{W}\approx 0.990\,34$ on the $K_1=20$ sector. The overlap with the Laughlin state $\mathcal{O}=|\langle\Psi_{\rm Lau}^{K_1=20}|\Psi^{J_1=2}(\lambda)\rangle|^2$ is 0.986 67. (f) The unprojected $|\Psi^{J_1=4}(\lambda)\rangle$ has weight $\mathcal{W}\approx 0.990\,34$ on the $K_1=4$ sector. The overlap with the Laughlin state $\mathcal{O}=|\langle\Psi_{\rm Lau}^{K_1=4}|\Psi^{J_1=4}(\lambda)\rangle|^2$ is 0.986 67. The weight and overlap in the middle and right columns are always the same because of the inversion symmetry of the Wannier basis (Ref. 23). The orange shadows indicate the generic levels in the OES of $|\Psi_{\rm prj}^{J_1}(\lambda)\rangle$, which deviate from the levels of the exact Laughlin state.

Considering that the structure of the Hilbert space does not change during the interpolation, we can make a cut in the basis and extract the OES of $|\Psi^i(\lambda)\rangle$ by the same method as that for FQH states. For pure FCI states, this corresponds to a cut in the localized Wannier orbitals. However, the total momentum K_1 in $|\Psi^i(\lambda)\rangle$ is not a good quantum number (except at $\lambda=0$). This means $|\Psi^i(\lambda)\rangle$ may have weight on some K_1 that $|\Psi_{\rm FQH}\rangle$ does not have weight on. We can calculate the weight $\mathcal{W}^i$ of each $|\Psi^i(\lambda)\rangle$ on the K_1 sectors of FQH states and obtain an average weight $\overline{\mathcal{W}}=\frac{1}{d}\sum_{i=1}^{d}\mathcal{W}^i$. From Fig. 2(b), we can see that the $|\Psi^i(\lambda>0)\rangle$ indeed has some "momentum leakage" leading to $\overline{\mathcal{W}}<1$. However, even for the pure FCI states at $\lambda=1$, K_1 is also almost conserved ($\overline{\mathcal{W}}\approx 0.990$ for $N_e=8$). Therefore, we project $|\Psi^i(\lambda)\rangle$ into the K_1 sector of the corresponding FQH states and consider the OES of $|\Psi_{\rm prj}^i(\lambda)\rangle$.

In Fig. 3, we display our OES results for $N_e=8$ (the lattice size is $N_1\times N_2=4\times 6$ for the FCI part). For this system size, $|\Psi^i(\lambda)\rangle$ are located in the $J_1=0$, $J_1=2$, and $J_1=4$ sectors. They correspond to the Laughlin state with the $K_1=12$ (100 sector), $K_1=20$ (010 sector), and $K_1=4$ (001 sector), respectively. We find that the OES almost perfectly match those of the corresponding Laughlin states up to $\xi=\xi_{\rm max}$ for all of the three $|\Psi^i(\lambda)\rangle$: $\xi_{\rm max}\approx 13.3$ at $\lambda=0.5$, while it reduces slightly to about 12.3 at $\lambda=1$. While the notion of an entanglement gap[26,35] can not be defined as crisply as in geometries with only one edge,[35,36] the impressive match of the OES with the model state nevertheless strongly suggests that the edge excitation properties of the Laughlin states are preserved during the interpolation and furthermore corroborates the adiabatic continuity between FCI states and FQH states at $\nu=\frac{1}{3}$. In Ref. 31, the OES of the $\nu=\frac{1}{3}$ Coulomb ground states were investigated and compared to the model states. In this case, there was a match of the OES levels with exact $\nu=\frac{1}{3}$ Laughlin state up to $\xi_{\rm max}\approx 8$ (the number of levels below this value increase with system size). That we find higher $\xi_{\rm max}$ here indicates that the FCI states in the lattice are actually closer to the Laughlin model states than is the case for the Coulomb FQH ground states.

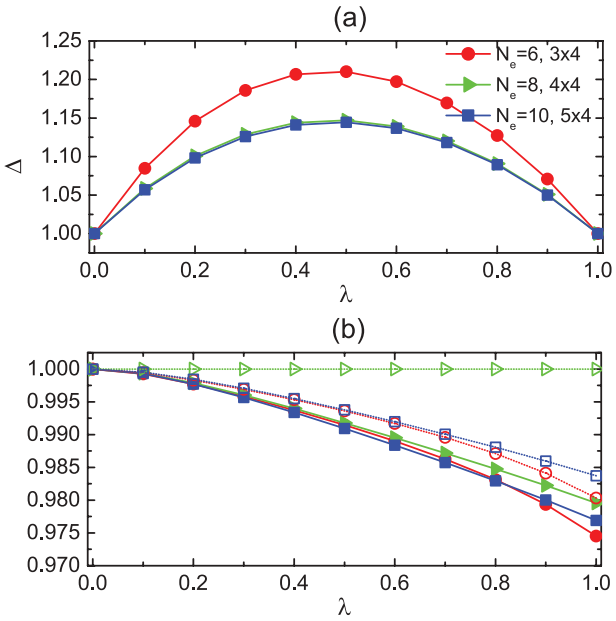

FIG. 4. (Color online) Results of the interpolation Eq. (4) for fermions at $\nu = \frac{1}{2}$ for $N_e = 6$ (red dot), $N_e = 8$ (green triangle), and $N_e = 10$ (blue square). In the FCI part, the lattice size is $N_1 \times N_2 = 3 \times 4$, $N_1 \times N_2 = 4 \times 4$, and $N_1 \times N_2 = 5 \times 4$, respectively; and $\lambda_1 = 0.8$. (a) The energy gap Δ does not close for any intermediate λ. (b) The total overlap $\mathcal{O}_{\rm tot}$ (filled symbol, solid line) and the average weight $\overline{\mathcal{W}}$ (empty symbol, dotted line) are still close to 1 at $\lambda = 1$. All of those demonstrate that the continuity holds for fermions at $\nu = \frac{1}{2}$. (One may note that for $N_e = 8$, $N_1 \times N_2 = 4 \times 4$, $\overline{\mathcal{W}} = 1$ for all λ. This is accidental for this particular lattice size.)

B. Fermions at $\nu = \frac{1}{2}$

It is also interesting to investigate whether the adiabatic continuity holds also for some non-Abelian states. In fact, none of the two previous Wannier basis studies[22,23] considered states in this class. To this end, we turn our attention to the $\nu = \frac{1}{2}$ fermionic Moore-Read phase. To obtain the exact fermionic Moore-Read states in the continuum on the torus, we choose $H_{\rm FQH} = \sum_{i<j<k} \mathcal{S}_{ijk} \nabla_i^2 \nabla_j^4 \delta^2(\mathbf{r}_i - \mathbf{r}_j) \delta^2(\mathbf{r}_j - \mathbf{r}_k)$, where $\mathcal{S}_{ijk}$ is the symmetrizing operator. The ground states are exact sixfold-degenerate fermionic Moore-Read states with zero energy. On the FCI side, we construct the Hamiltonian as a three-body interaction $H_{\rm FCI} = \sum_{\langle ijk \rangle} n_i n_j n_k$ between three nearest-neighbor sites. The ground states are six nearly degenerate states separated by a gap from the excited states. Here, we choose a different twisted angle $\alpha = 2\pi/3$ for the torus and this is justified by the large overlap between the FCI states at $\lambda = 1$ and the Moore-Read states at $\lambda = 0$ (for $\alpha = \pi/3$, this overlap is relatively small).

We find that there are six nearly degenerate states $|\Psi^i(\lambda)\rangle$ for each $\lambda \in [0,1]$. The evolution of the energy gap [Fig. 4(a)], total overlap, and average weight [Fig. 4(b)] behave similarly with those for the $\nu = \frac{1}{3}$ fermionic Laughlin phase. While both of the total overlap and average weight are slightly smaller ($\mathcal{O}_{\rm tot} \approx 0.977$ and $\overline{\mathcal{W}} \approx 0.984$ at $\lambda = 1$ for our largest system size $N_e = 10$), these numbers are way above the overlaps found between the Moore-Read state and the Coulomb ground state in the second Landau level.[37] (Of course, the three-body lattice Hamiltonian used here for the FCI is somewhat artificial to begin with, making a direct comparison of overlaps a bit biased.)

We also consider the OES for $N_e = 10$ (the lattice size is $N_1 \times N_2 = 5 \times 4$ for the FCI part). In the continuum, the thin-torus configuration of the six fermionic Moore-Read states are[38] (for $N_e = 10$, $N_s = 20$)

$$010101|\mathbf{0101010101}|0101,$$
$$101010|\mathbf{1010101010}|1010,$$
$$01100|\mathbf{1100110011}|00110 \pm 10011|\mathbf{0011001100}|11001,$$
$$11001|\mathbf{1001100110}|01100 \pm 00110|\mathbf{0110011001}|10011.$$

Their total momentum is $K_1 = 0$, $K_1 = 10$, $K_1 = 15$ (twofold), and $K_1 = 5$ (twofold), respectively. Among the six $|\Psi^i(\lambda)\rangle$, one is located in the $J_1 = 0$ sector [corresponding to the $K_1 = 0$ Moore-Read state (0101 sector)], one is located in the $J_1 = 2$ sector [corresponding to the $K_1 = 10$ Moore-Read state (1010 sector)], two are located in the $J_1 = 1$ sector [corresponding to the two $K_1 = 5$ Moore-Read states (1100 ± 0011 sectors)], and two are located in the $K_2 = 3$ sector [corresponding to the two $K_1 = 15$ Moore-Read states (0110 ± 1001 sectors)]. The two $|\Psi^i(\lambda)\rangle$ with the same $J_1 = 1$ ($J_1 = 3$) will mix with each other, so they do not have a one-to-one correspondence to the $1100 + 0011$ state and $1100 - 0011$ state ($0110 + 1001$ state and $0110 - 1001$ state). Therefore, we only consider the OES for the $|\Psi^i(\lambda)\rangle$ in the $J_1 = 0$ and $J_1 = 2$ sectors here by projecting them into the K_1 sector of the corresponding Moore-Read states. In Fig. 5, we can see that the low-lying part of the OES of $|\Psi^i_{\rm prj}(\lambda)\rangle$ also matches that of the exact Moore-Read state very well. As expected, $\xi_{\rm max}$ here ($\xi_{\rm max} \approx 12.5$ at $\lambda = 0.5$ and $\xi_{\rm max} \approx 11$ at $\lambda = 1$) is lower slightly than that for the $\nu = \frac{1}{3}$ fermionic Laughlin case reflecting the lower overlap. We also find that the OES of $|\Psi^i_{\rm prj}(\lambda)\rangle$ lack inversion (left-right) symmetry, which is not so obvious in the $\nu = \frac{1}{3}$ state. However, taken together there is no doubt that the FCI phase is excellently described by the Moore-Read wave function, and the low-energy physics of the FCI problem should thus be within the same universality class.

C. Fermions at $\nu = \frac{4}{5}$ and $\nu = \frac{2}{3}$

Finally, we consider a case where there is a lack of adiabatic continuity between the low-energy sector of the FQH and FCI Hamiltonians. To this end, we focus on fermions at $\nu = \frac{4}{5}$. On the FQH side, we choose the Hamiltonian as $H_{\rm FQH} = \sum_{i<j} \nabla_i^6 \delta^2(\mathbf{r}_i - \mathbf{r}_j)$. Then, the ground states are fivefold-degenerate states that are the particle-hole conjugate (phc) of $\nu = \frac{1}{5}$ Laughlin states. On the FCI side, the Hamiltonian is set as the nearest-neighbor interaction $H_{\rm FCI} = \sum_{\langle ij \rangle} n_i n_j$. Due to the particle-hole symmetry breaking, the ground states are no longer FCI states but competing compressible (fermion-liquid-like) states without the fivefold nearly degeneracy.[15] Here, we set $\beta = \pi/3$, $w_{\rm FCI} = w_{\rm FQH} = 1$, and choose $|\Psi^i(\lambda)\rangle$ as the ground states in the J_1 sectors where the FQH states are located in at $\lambda = 0$. We use the total overlap and OES to probe the phase transition between $\lambda = 0$ and 1. In Fig. 6, it is clear that the total overlap drops down to a very small number at intermediate λ. In Fig. 7, we choose the $|\Psi^i(\lambda)\rangle$ in the $J_1 = 2$ sector to study the OES. One can see that the OES

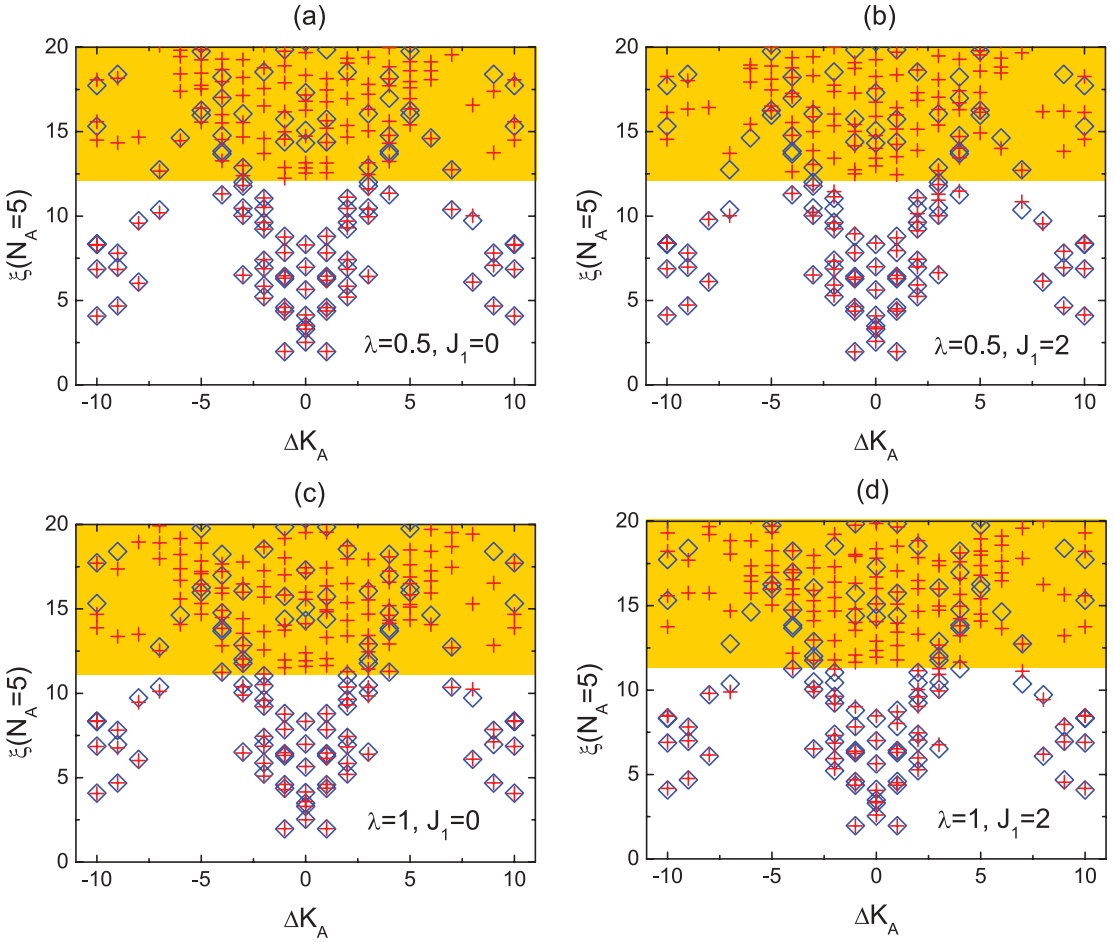

FIG. 5. (Color online) The orbital entanglement spectra (OES) of exact fermionic Moore-Read states (blue diamond) and the projected nearly degenerate states $|\Psi^{J_1}_{\rm prj}(\lambda)\rangle$ (red cross) at $\nu = \frac{1}{2}$, $N_e = 10$. The lattice size is $N_1 \times N_2 = 5 \times 4$ and $\lambda_1 = 0.8$ for the FCI part. In the left column, $J_1 = 0$, corresponding to the Moore-Read state in the $K_1 = 0$ sector. In the right column, $J_1 = 2$, corresponding to the Moore-Read state in the $K_1 = 10$ sector. In (a) and (b), $\lambda = 0.5$. (a) The unprojected $|\Psi^{J_1=0}(\lambda)\rangle$ has weight $\mathcal{W} \approx 0.994\,03$ on the $K_1 = 0$ sector. The overlap with the Moore-Read state $\mathcal{O} = |\langle\Psi^{K_1=0}_{\rm MR}|\Psi^{J_1=0}(\lambda)\rangle|^2$ is 0.991 19. (b) The unprojected $|\Psi^{J_1=2}(\lambda)\rangle$ has weight $\mathcal{W} \approx 0.994\,36$ on the $K_1 = 10$ sector. The overlap with the Moore-Read state $\mathcal{O} = |\langle\Psi^{K_1=10}_{\rm MR}|\Psi^{J_1=2}(\lambda)\rangle|^2$ is 0.990 94. In (c) and (d), $\lambda = 1$. (c) The unprojected $|\Psi^{J_1=0}(\lambda)\rangle$ has weight $\mathcal{W} \approx 0.984\,88$ on the $K_1 = 0$ sector. The overlap with the Moore-Read state $\mathcal{O} = |\langle\Psi^{K_1=0}_{\rm MR}|\Psi^{J_1=0}(\lambda)\rangle|^2$ is 0.977 92. (d) The unprojected $|\Psi^{J_1=2}(\lambda)\rangle$ has weight $\mathcal{W} \approx 0.985\,83$ on the $K_1 = 10$ sector. The overlap with the Moore-Read state $\mathcal{O} = |\langle\Psi^{K_1=10}_{\rm MR}|\Psi^{J_1=2}(\lambda)\rangle|^2$ is 0.977 50. The orange shadows indicate the generic levels in the OES of $|\Psi^{J_1}_{\rm prj}(\lambda)\rangle$, which deviate from the levels of the exact Moore-Read state.

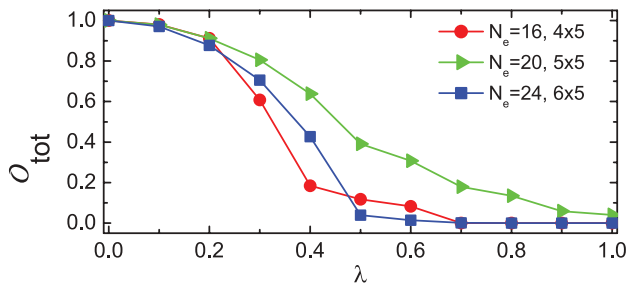

FIG. 6. (Color online) Results of the interpolation Eq. (4) for fermions at $\nu = \frac{4}{5}$ for $N_e = 16$ (red dot), $N_e = 20$ (green triangle), and $N_e = 24$ (blue square). In the FCI part, the lattice size is $N_1 \times N_2 = 4 \times 5$, $N_1 \times N_2 = 5 \times 5$, and $N_1 \times N_2 = 6 \times 5$, respectively; and $\lambda_1 = 1$. The total overlap $\mathcal{O}_{\rm tot}$ shows a clear drop at intermediate λ, which demonstrates that the continuity does not hold for fermions at $\nu = \frac{4}{5}$.

of the projected $|\Psi^i(\lambda)\rangle$ match those of the corresponding phc FQH state up to $\xi_{\rm max} \approx 10$ at $\lambda = 0.1$, but completely deviate at $\lambda = 0.5$. Our results clearly show that the adiabatic continuity indeed does not hold for fermions at $\nu = \frac{4}{5}$.

We also find a similar phase transition for fermions at $\nu = \frac{2}{3}$. However, $\nu = \frac{2}{3}$ is probably on the border between competing compressible states and FCI states (see Ref. 15 for such study in checkerboard lattice), thus it is quite likely that the appearance of this phase transition may depend on the system size and the shape of the samples. On the contrary, we expect the $\nu = \frac{4}{5}$ results showing a clear phase transition to be robust to such details.

IV. DISCUSSION

In this paper, we have investigated the interpolation between the FCI states and FQH states with the help of appropriately

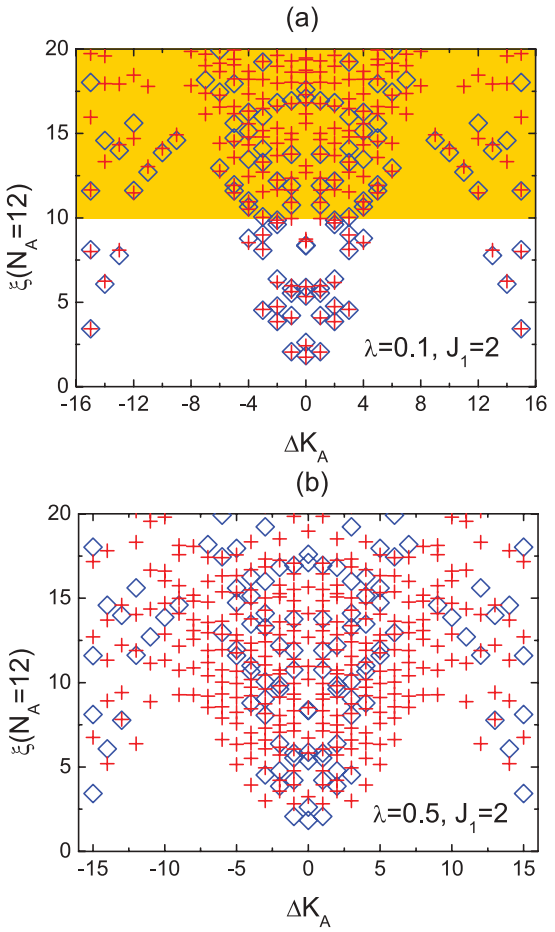

FIG. 7. (Color online) The orbital entanglement spectra (OES) of exact fermionic phc state (blue diamond) and the projected state $|\Psi^{J_1}_{\rm prj}(\lambda)\rangle$ (red cross) at $\nu = \frac{4}{5}$, $N_e = 24$. $|\Psi^{J_1}_{\rm prj}(\lambda)\rangle$ is in the $J_1 = 2$ sector and corresponds to the phc state in the $K_1 = 12$ sector. The lattice size is $N_1 \times N_2 = 6 \times 5$ and $\lambda_1 = 1$ for the FCI part. (a) $\lambda = 0.1$. The unprojected $|\Psi^{J_1}(\lambda)\rangle$ has weight $\mathcal{W} \approx 0.986\,45$ on the $K_1 = 12$ sector. The overlap with the phc state $\mathcal{O} = |\langle\Psi^{K_1=12}_{\rm phc}|\Psi^{J_1=2}(\lambda)\rangle|^2$ is 0.972 13. (b) $\lambda = 0.5$. The unprojected $|\Psi^{J_1}(\lambda)\rangle$ has weight $\mathcal{W} \approx 0.067\,92$ on the $K_1 = 12$ sector. The overlap with the phc state $\mathcal{O} = |\langle\Psi^{K_1=12}_{\rm phc}|\Psi^{J_1=2}(\lambda)\rangle|^2$ is almost 0.

gauge-fixed Wannier wave functions.[21,23] By demonstrating an almost constant gap and a large overlap during the interpolation, we provide the strong evidence that both Abelian and non-Abelian FCI states are adiabatically connected to their corresponding FQH (Laughlin and Moore-Read, respectively) states for fermions as well as for bosons. The method used here may be seen as an improved version of the first study of adiabatic continuity,[22] which studied $\nu = \frac{1}{2}$ bosons, by utilizing the recent gauge-fixing insights of Ref. 23. It also provides a more direct and quantitative comparison between FCI and FQH than the likewise elegant connection recently established via relating Chern bands to the Landau bands of the Hofstadter problem in Ref. 39.

To underscore the nontriviality of our results, we have also considered fermions at filling factor $\nu = \frac{4}{5}$, for which there is no FCI state due to the particle-hole symmetry breaking[15] in the Chern band (this symmetry breaking is absent in a

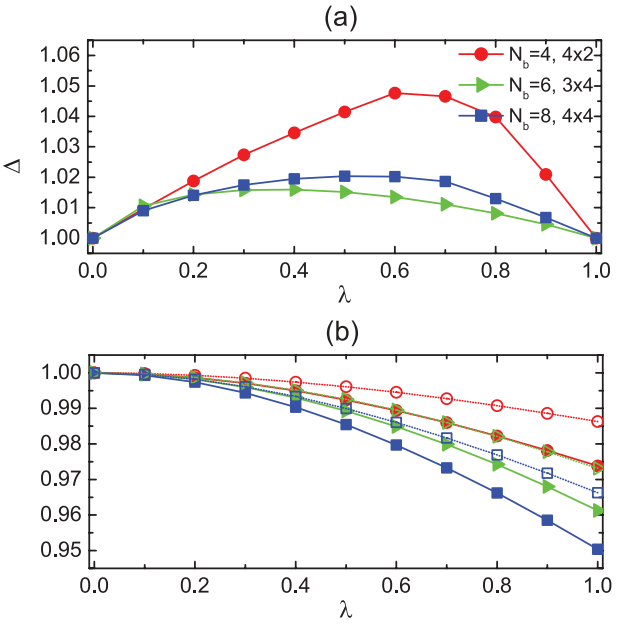

FIG. 8. (Color online) Results of the interpolation Eq. (4) for bosons at $\nu = \frac{1}{2}$ for $N_b = 4$ (red dot), $N_b = 6$ (green triangle), and $N_b = 8$ (blue square). In the FCI part, the lattice size is $N_1 \times N_2 = 4 \times 2$, $N_1 \times N_2 = 3 \times 4$, and $N_1 \times N_2 = 4 \times 4$, respectively; and $\lambda_1 = 1$. (a) The energy gap Δ does not close for any intermediate λ. (b) The total overlap $\mathcal{O}_{\rm tot}$ (filled symbol, solid line) and the average weight $\overline{\mathcal{W}}$ (empty symbol, dotted line) are still close to 1 at $\lambda = 1$. All of those demonstrate that the continuity holds for bosons at $\nu = \frac{1}{2}$.

Landau level). The overlap and gap indeed drop drastically during the interpolation, reflecting a phase transition. In Ref. 40, it was pointed out that the particle-hole symmetry can be explicitly restored by adding a single-particle term to the standard normal-ordered Hamiltonian $H_{\rm FCI}$, which is used in most numerical studies including this work.[41] By examining the adiabatic continuity using the resulting particle-hole-symmetric FCI Hamiltonian, we find that the results are significantly less universal and that they crucially depend on details such as the system size, the tight-binding parameters, and the interaction we choose.

We have also given a report of the orbital entanglement spectrum (OES) of FCI states based on the orbital cut in the localized Wannier basis. The low-lying parts of the OES of FCI states match those of corresponding ideal model FQH states very well. By comparing the OES of FCI states with those of FQH states obtained from realistic interaction in Landau levels, we find that FCI states are closer to the ideal FQH states. The analysis of the OES generalizes earlier works on FQH states on the torus, and thereby provides an appealing picture of the FCI OES as composed of two CFT spectra with opposite chirality.[31,32] Invoking the bulk-edge correspondence,[26,42–44] our results also provide a glimpse of the gapless edge physics of the FCI phases.

Our work invites a number of interesting future directions. Perhaps most interestingly, it suggests a natural generalization studying FCI states in Chern bands with higher Chern number. Indeed, novel series of FCI states with arbitrary Chern number $|\mathcal{C}| = N$ have recently been observed in numerics.[45,46] While these new states might correspond to appropriately

symmetrized versions of multicomponent FQH states,[45–47] such ideas need to be substantiated by further investigations and more direct comparisons as would be possible within the framework used here.

Another important issue would be if the present formalism might have bearing for the development of a pseudopotential formalism for fractional Chern insulators. At present, there are two approaches,[15,48] one of which is built on the original (non-gauge-fixed) Wannier basis construction,[48] leading to apparently diverging predictions.

ACKNOWLEDGMENTS

We acknowledge A. Läuchli for several related collaborations. E.J.B. is supported by the Alexander von Humboldt foundation. Z.L. is supported by the China Postdoctoral Science Foundation Grant No. 2012M520149.

APPENDIX A: BOSONS AT $\nu = \frac{1}{2}$

In this section, we focus on the continuity problem of bosons at filling factor $\nu = \frac{1}{2}$. On the FQH side, we choose the Hamiltonian as $H_{\mathrm{FQH}} = \sum_{i<j} \delta^2(\mathbf{r}_i - \mathbf{r}_j)$. Then, the ground states are exact twofold-degenerate bosonic Laughlin states with zero energy. On the FCI side, the Hamiltonian is set as the onsite interaction $H_{\mathrm{FCI}} = \sum_i n_i(n_i - 1)$. The ground states are two nearly degenerate states separated by a gap from the excited states. We set $\alpha = \pi/3$ also for the twisted torus.

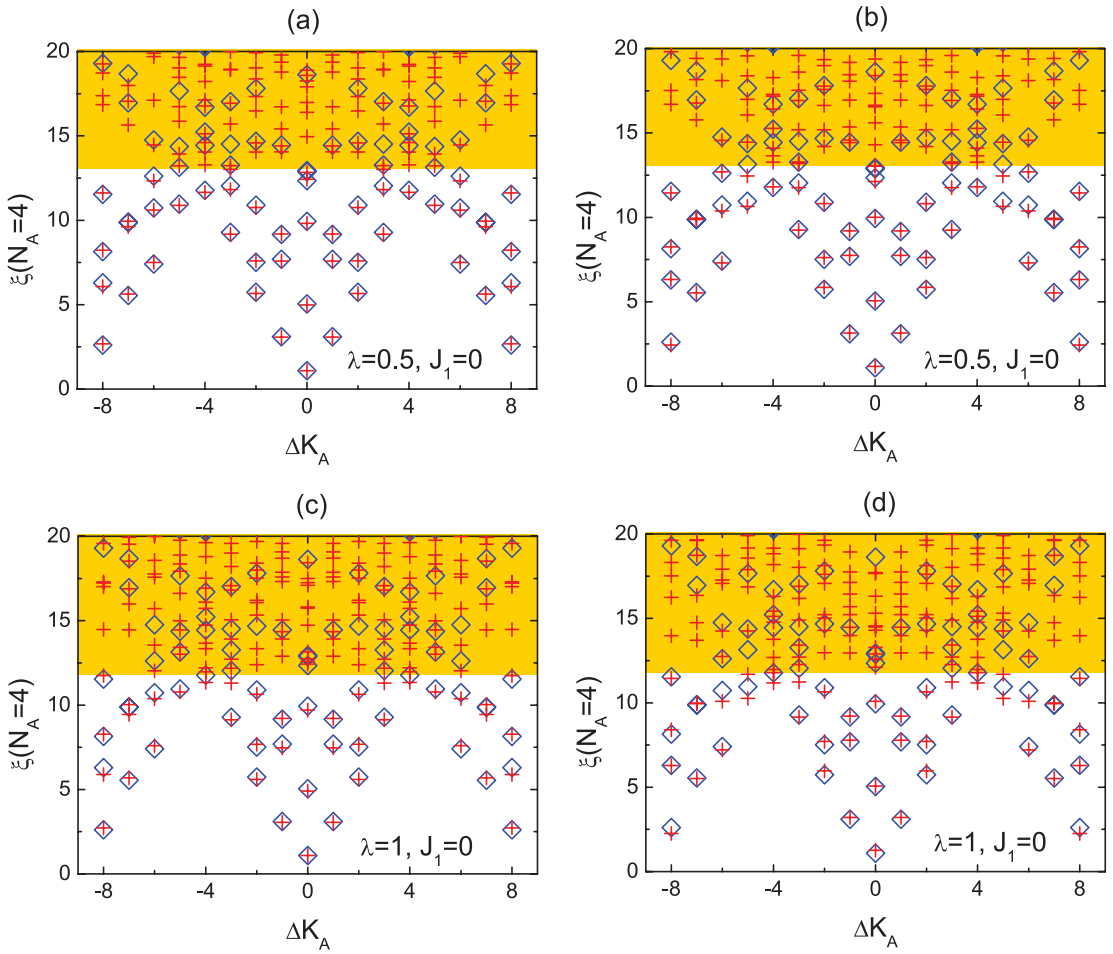

FIG. 9. (Color online) The orbital entanglement spectra (OES) of exact bosonic Laughlin states (blue diamond) and the projected nearly degenerate states $|\Psi^{J_1}_{\mathrm{prj}}(\lambda)\rangle$ (red cross) at $\nu = \frac{1}{2}$, $N_b = 8$. The lattice size is $N_1 \times N_2 = 4 \times 4$ and $\lambda_1 = 1$ for the FCI part. Both of the two nearly degenerate states are in the $J_1 = 0$ sector. In the left column, we consider the one with lower energy and project it in the $K_1 = 0$ sector. In the right column, we consider the one with higher energy and project it in the $K_1 = 8$ sector. In (a) and (b), $\lambda = 0.5$. (a) The unprojected $|\Psi^{J_1}(\lambda)\rangle$ has weight $\mathcal{W} \approx 0.797\,21$ on the $K_1 = 0$ sector and $\mathcal{W} \approx 0.190\,96$ on the $K_1 = 8$ sector. The overlap with the Laughlin state $\mathcal{O} = \frac{1}{2}(|\langle\Psi^{K_1=0}_{\mathrm{Lau}}|\Psi^{J_1=0}(\lambda)\rangle|^2 + |\langle\Psi^{K_1=8}_{\mathrm{Lau}}|\Psi^{J_1=0}(\lambda)\rangle|^2)$ is 0.982 64. (b) The unprojected $|\Psi^{J_1}(\lambda)\rangle$ has weight $\mathcal{W} \approx 0.192\,76$ on the $K_1 = 0$ sector and $\mathcal{W} \approx 0.799\,02$ on the $K_1 = 8$ sector. The overlap with the Laughlin state $\mathcal{O} = \frac{1}{2}(|\langle\Psi^{K_1=0}_{\mathrm{Lau}}|\Psi^{J_1=0}(\lambda)\rangle|^2 + |\langle\Psi^{K_1=8}_{\mathrm{Lau}}|\Psi^{J_1=0}(\lambda)\rangle|^2)$ is 0.988 25. In (c) and (d), $\lambda = 1$. (c) The unprojected $|\Psi^{J_1}(\lambda)\rangle$ has weight $\mathcal{W} \approx 0.759\,66$ on the $K_1 = 0$ sector and $\mathcal{W} \approx 0.199\,68$ on the $K_1 = 8$ sector. The overlap with the Laughlin state $\mathcal{O} = \frac{1}{2}(|\langle\Psi^{K_1=0}_{\mathrm{Lau}}|\Psi^{J_1=0}(\lambda)\rangle|^2 + |\langle\Psi^{K_1=8}_{\mathrm{Lau}}|\Psi^{J_1=0}(\lambda)\rangle|^2)$ is 0.939 67. (d) The unprojected $|\Psi^{J_1}(\lambda)\rangle$ has weight $\mathcal{W} \approx 0.206\,03$ on the $K_1 = 0$ sector and $\mathcal{W} \approx 0.767\,20$ on the $K_1 = 8$ sector. The overlap with the Laughlin state $\mathcal{O} = \frac{1}{2}(|\langle\Psi^{K_1=0}_{\mathrm{Lau}}|\Psi^{J_1=0}(\lambda)\rangle|^2 + |\langle\Psi^{K_1=8}_{\mathrm{Lau}}|\Psi^{J_1=0}(\lambda)\rangle|^2)$ is 0.961 11. The orange shadows indicate the generic levels in the OES of $|\Psi^{J_1}_{\mathrm{prj}}(\lambda)\rangle$, which deviate from the levels of the exact Laughlin state.

We find that there are two nearly degenerate states $|\Psi^i(\lambda)\rangle$ for each $\lambda \in [0,1]$. The evolution of the energy gap [Fig. 8(a)], total overlap, and average weight [Fig. 8(b)] is similar with that for the $\nu = \frac{1}{3}$ fermionic Laughlin phase. However, both of the total overlap and average weight are smaller ($\mathcal{O}_{\rm tot} \approx 0.950$ and $\overline{\mathcal{W}} \approx 0.9663$ at $\lambda = 1$ for our largest system size $N_b = 8$).

We consider the OES for $N_b = 8$ (the lattice size is $N_1 \times N_2 = 4 \times 4$ for the FCI part). In the continuum, the thin-torus configuration of the two bosonic Laughlin states are (for $N_b = 8$, $N_s = 16$)

$$0101|\mathbf{01010101}|0101,$$
$$1010|\mathbf{10101010}|1010.$$

Their total momentum is $K_1 = 0$ and 8, respectively. The two $|\Psi^i(\lambda)\rangle$ are both in the $J_1 = 0$ sector, so they mix with each other and do not have a good one-to-one correspondence with the two Laughlin states. This means that each $|\Psi^i(\lambda)\rangle$ has weight on the $K_1 = 0$ and 8 sectors simultaneously. However, we can still project one $|\Psi^i(\lambda)\rangle$ in the $K_1 = 0$ sector and project the other in the $K_1 = 8$ sector. In Fig. 9, we can see that the low-lying part of the OES of $|\Psi^i_{\rm prj}(\lambda)\rangle$ also matches that of the exact Laughlin state very well. Of course, $\xi_{\rm max}$ here ($\xi_{\rm max} \approx 13.2$ at $\lambda = 0.5$ and $\xi_{\rm max} \approx 11.2$ at $\lambda = 1$) is lower than that in the $\nu = \frac{1}{3}$ fermionic Laughlin case due to the lower overlap. However, all of our results strongly support that the FQH states are adiabatically connected to FCI states for bosons at $\nu = \frac{1}{2}$.

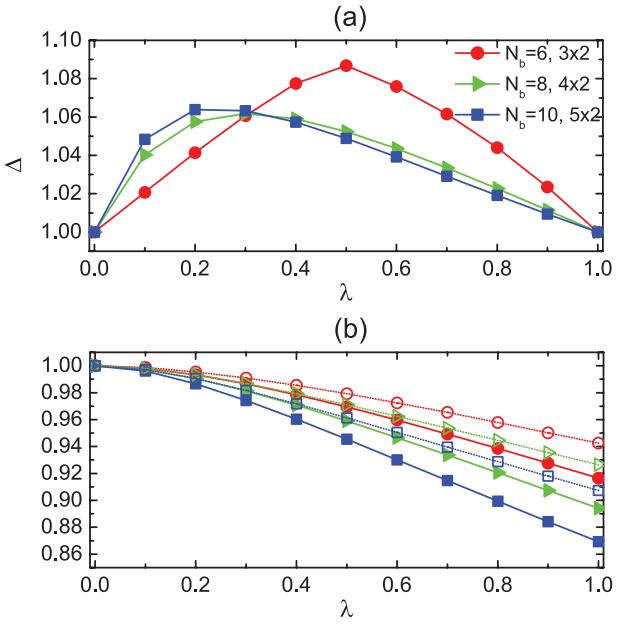

FIG. 10. (Color online) Results of the interpolation Eq. (4) for bosons at $\nu = 1$ for $N_b = 6$ (red dot), $N_b = 8$ (green triangle), and $N_b = 10$ (blue square). In the FCI part, the lattice size is $N_1 \times N_2 = 3 \times 2$, $N_1 \times N_2 = 4 \times 2$, and $N_1 \times N_2 = 5 \times 2$, respectively; and $\lambda_1 = 0.8$. (a) The energy gap Δ does not close for any intermediate λ. (b) The total overlap $\mathcal{O}_{\rm tot}$ (filled symbol, solid line) and the average weight $\overline{\mathcal{W}}$ (empty symbol, dotted line) are still large at $\lambda = 1$. All of those demonstrate that the continuity holds for bosons at $\nu = 1$.

APPENDIX B: BOSONS AT $\nu = 1$

In this section, we focus on the continuity problem of bosons at filling factor $\nu = 1$. On the FQH side, we choose the Hamiltonian as $H_{\rm FQH} = \sum_{i<j<k} \delta^2(\mathbf{r}_i - \mathbf{r}_j)\delta^2(\mathbf{r}_j - \mathbf{r}_k)$. Then, the ground states are exact threefold-degenerate bosonic Laughlin states with zero energy. On the FCI side, the Hamiltonian is tactically chosen as the onsite three-body interaction $H_{\rm FCI} = \sum_i n_i(n_i - 1)(n_i - 2)$. The ground states are three nearly degenerate states separated by a gap from the excited states. We set $\alpha = 2\pi/3$ for the twisted torus as was done for the fermion case at $\nu = \frac{1}{2}$.

We find that there are three nearly degenerate states $|\Psi^i(\lambda)\rangle$ for each $\lambda \in [0,1]$. The evolution of the energy gap [Fig. 10(a)], total overlap, and average weight [Fig. 10(b)] is similar with

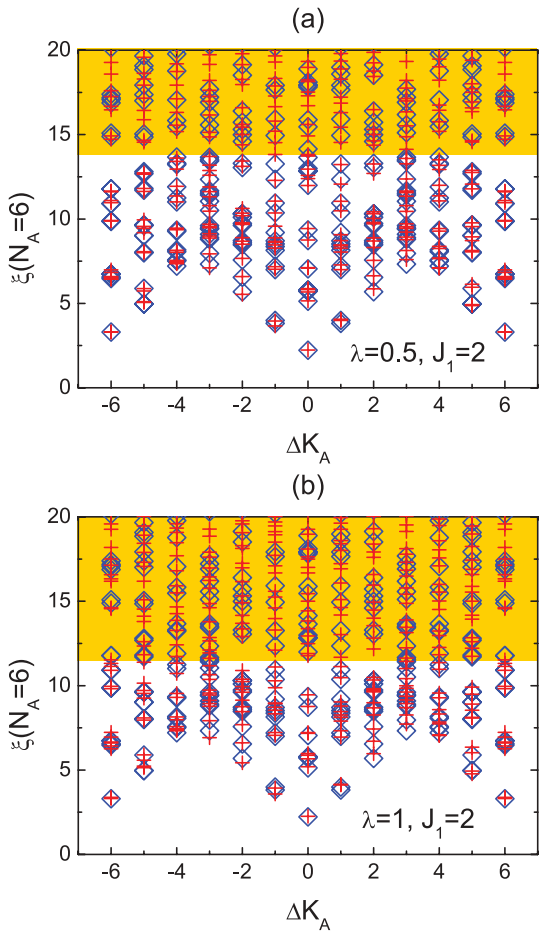

FIG. 11. (Color online) The orbital entanglement spectra (OES) of exact bosonic Moore-Read states (blue diamond) and the projected nearly degenerate state $|\Psi^{J_1}_{\rm prj}(\lambda)\rangle$ (red cross) at $\nu = 1$, $N_b = 12$. $|\Psi^{J_1}_{\rm prj}(\lambda)\rangle$ is in the $J_1 = 2$ sector and corresponds to the Moore-Read state in the $K_1 = 6$ sector. The lattice size is $N_1 \times N_2 = 3 \times 4$ and $\lambda_1 = 0.8$ for the FCI part. (a) $\lambda = 0.5$. The unprojected $|\Psi^{J_1}(\lambda)\rangle$ has weight $\mathcal{W} \approx 0.958\,60$ on the $K_1 = 6$ sector. The overlap with the Moore-Read state $\mathcal{O} = |\langle\Psi^{K_1=6}_{\rm MR}|\Psi^{J_1=2}(\lambda)\rangle|^2$ is 0.937 07. (b) $\lambda = 1$. The unprojected $|\Psi^{J_1}(\lambda)\rangle$ has weight $\mathcal{W} \approx 0.895\,28$ on the $K_1 = 6$ sector. The overlap with the Moore-Read state $\mathcal{O} = |\langle\Psi^{K_1=6}_{\rm MR}|\Psi^{J_1=2}(\lambda)\rangle|^2$ is 0.839 76. The orange shadows indicate the generic levels in the OES of $|\Psi^{J_1}_{\rm prj}(\lambda)\rangle$, which deviate from the levels of the exact Moore-Read state.

that for the $\nu = \frac{1}{2}$ fermionic Moore-Read phase. However, both of the total overlap and average weight are smaller ($\mathcal{O}_{\rm tot} \approx 0.869$ and $\overline{\mathcal{W}} \approx 0.9073$ at $\lambda = 1$ for our largest system size $N_b = 10$).

We consider the OES for $N_b = 12$ (the lattice size is $N_1 \times N_2 = 3 \times 4$ for the FCI part). In the continuum, the thin-torus configuration of the two bosonic Laughlin states are (for $N_b = 12$, $N_s = 12$)

$$111|\mathbf{111111}|111,$$
$$020|\mathbf{202020}|202 \pm 202|\mathbf{020202}|020.$$

Their total momentum is $K_1 = 6$ and 0 (twofold). The three $|\Psi^i(\lambda)\rangle$ are in the $J_1 = 0$ sector (twofold) and $J_1 = 2$ sector. Because the two states in the $J_1 = 0$ sector will mix with each other, we only concentrate on the single state in the $J_1 = 2$ sector, which corresponds to the $K_1 = 6$ Moore-Read state. Compared with the fermionic Moore-Read case, the asymmetry problem in the OES is more serious (Fig. 11). Although the OES of $|\Psi^{J_1=2}(\lambda)\rangle$ do not precisely match those of the exact bosonic Moore-Read state, we can still find a relatively good correspondence between their OES levels up to $\xi_{\rm max} \approx 13.8$ at $\lambda = 0.5$ and $\xi_{\rm max} \approx 11.5$ at $\lambda = 1$.

APPENDIX C: FURTHER DETAILS ON THE WANNIER BASIS CONSTRUCTION

To make this paper self-contained, we give the prescription of how to fix the phases $\Phi(k_2)$ in the Wannier function $|X,k_2\rangle$ in this Appendix. The results were first found in Ref. 23. The essential point in fixing the phase is to make the connection $\langle X,k_2|\hat{Y}|X',k_2'\rangle$ between adjacent Wannier states independent of X and k_2. Here, $\hat{Y} = \sum_{k_1,k_2} |k_1,k_2\rangle A_2(k_1,k_2)\langle k_1,k_2+1|$ is the unitary projected position operator in the $\mathbf{e}_y$ direction, and adjacent Wannier states are defined by $j^{X',k_2'} = j^{X,k_2} + \mathcal{C}$. Because $j^{X,k_2} = N_2 X + \mathcal{C}k_2 + \delta_2$, $k_2' = k_2 + 1 \pmod{N_2}$ for two adjacent Wannier states. If increasing from k_2 to k_2+1 does not cross the boundary of pBZ, $X' = X$. Otherwise, $X' = X + \mathcal{C}$.

From the definition of the Wannier state, one can obtain that

$$\langle X,k_2|\hat{Y}|X',k_2'\rangle = e^{i[\Phi(k_2')-\Phi(k_2)]} A_2(0,k_2)\mathcal{U}_2(k_2), \tag{C1}$$

where

$$\mathcal{U}_2(k_2) = \frac{1}{N_1}\sum_{k_1=0}^{N_1-1} \frac{W(k_1,k_2)}{W'(k_1,k_2)}$$

with

$$W(k_1,k_2) = \frac{\prod_{\kappa=0}^{k_1-1} A_1(\kappa,k_2)}{\prod_{\kappa=0}^{k_1-1} A_1(\kappa,k_2+1)} \frac{A_2(k_1,k_2)}{A_2(0,k_2)},$$

$W'(k_1,k_2) = [\mu_1(k_2)]^{k_1}$, and

$$\mu_1(k_2) = \begin{cases} \frac{\lambda_1(k_2)}{\lambda_1(k_2+1)}, & k_2+1 \in \text{pBZ} \\ e^{2\pi i \mathcal{C}/N_1} \frac{\lambda_1(k_2)}{\lambda_1(k_2+1)}, & \text{otherwise.} \end{cases}$$

The product of $\langle X,k_2|\hat{Y}|X',k_2'\rangle$ has a very simple form

$$\prod_{X=0}^{N_1-1}\prod_{k_2=0}^{N_2-1} \langle X,k_2|\hat{Y}|X',k_2'\rangle = \left[W_2(0)\prod_{k_2=0}^{N_2-1}\mathcal{U}_2(k_2)\right]^{N_1}. \tag{C2}$$

Defining $U_2(k_2) = \mathcal{U}_2(k_2)/|\mathcal{U}_2(k_2)|$ and introducing a phase $(\omega_2)^{N_2} = \prod_{k_2=0}^{N_2-1} U_2(k_2)$ with the argument angle in $(-\pi/N_2, \pi/N_2)$, we can choose $\langle X,k_2|\hat{Y}|X',k_2'\rangle = \lambda_2(0)\omega_2|\mathcal{U}_2(k_2)|$, which satisfies Eq. (C2). Finally, by comparing this choice with Eq. (C1), we have

$$e^{i[\Phi(k_2')-\Phi(k_2)]} = \frac{\lambda_2(0)}{A_2(0,k_2)}\frac{\omega_2}{U_2(k_2)}. \tag{C3}$$

We can choose $e^{i\Phi(0)} = 1$ and recursively fix all phases $e^{i\Phi(k_2)}$ according to Eq. (C3).

*zliu@csrc.ac.cn
†ejb@physik.fu-berlin.de

[1] F. D. M. Haldane, Phys. Rev. Lett. **61**, 2015 (1988).
[2] E. Tang, J.-W. Mei, and X.-G. Wen, Phys. Rev. Lett. **106**, 236802 (2011).
[3] K. Sun, Z. Gu, H. Katsura, and S. Das Sarma, Phys. Rev. Lett. **106**, 236803 (2011).
[4] T. Neupert, L. Santos, C. Chamon, and C. Mudry, Phys. Rev. Lett. **106**, 236804 (2011).
[5] D. N. Sheng, Z. Gu, K. Sun, and L. Sheng, Nat. Commun. **2**, 389 (2011).
[6] N. Regnault and B. A. Bernevig, Phys. Rev. X **1**, 021014 (2011).
[7] J. W. F. Venderbos, M. Daghofer, and J. van den Brink, Phys. Rev. Lett. **107**, 116401 (2011).
[8] D. Xiao, W. Zhu, Y. Ran, N. Nagaosa, and S. Okamoto, Nat. Commun. **2**, 596 (2011).
[9] F. Wang and Y. Ran, Phys. Rev. B **84**, 241103(R) (2011).
[10] J. W. F. Venderbos, S. Kourtis, J. van den Brink, and M. Daghofer, Phys. Rev. Lett. **108**, 126405 (2012).
[11] P. Ghaemi, J. Cayssol, D. N. Sheng, and A. Vishwanath, Phys. Rev. Lett. **108**, 266801 (2012).
[12] M. Trescher and E. J. Bergholtz, Phys. Rev. B **86**, 241111(R) (2012).
[13] N. Y. Yao, C. R. Laumann, A. V. Gorshkov, S. D. Bennett, E. Demler, P. Zoller, and M. D. Lukin, Phys. Rev. Lett. **109**, 266804 (2012).
[14] T. Liu, C. Repellin, B. A. Bernevig, and N. Regnault, arXiv:1206.2626.
[15] A. Läuchli, Z. Liu, E. J. Bergholtz, and R. Moessner, arXiv:1207.6094.
[16] S. Kourtis, J. W. F. Venderbos, and M. Daghofer, Phys. Rev. B **86**, 235118 (2012).
[17] B. A. Bernevig and N. Regnault, Phys. Rev. B **85**, 075128 (2012).
[18] Y.-F. Wang, H. Yao, Z.-C. Gu, C.-D. Gong, and D. N. Sheng, Phys. Rev. Lett. **108**, 126805 (2012).
[19] Y.-L. Wu, B. A. Bernevig, and N. Regnault, Phys. Rev. B **85**, 075116 (2012).
[20] S. A. Parameswaran, R. Roy, and S. L. Sondhi, Phys. Rev. B **85**, 241308(R) (2012); M. O. Goerbig, Eur. Phys. J. B **85**, 15 (2012); R. Roy, arXiv:1208.2055.
[21] X.-L. Qi, Phys. Rev. Lett. **107**, 126803 (2011).
[22] T. Scaffidi and G. Möller, Phys. Rev. Lett. **109**, 246805 (2012).

[23] Y.-L. Wu, N. Regnault, and B. A. Bernevig, Phys. Rev. B **86**, 085129 (2012).
[24] R. B. Laughlin, Phys. Rev. Lett. **50**, 1395 (1983).
[25] G. Moore and N. Read, Nucl. Phys. B **360**, 362 (1991).
[26] H. Li and F. D. M. Haldane, Phys. Rev. Lett. **101**, 010504 (2008).
[27] A. Sterdyniak, N. Regnault, and B. A. Bernevig, Phys. Rev. Lett. **106**, 100405 (2011).
[28] M. Haque, O. Zozulya, and K. Schoutens, Phys. Rev. Lett. **98**, 060401 (2007).
[29] F. D. M. Haldane, Phys. Rev. Lett. **55**, 2095 (1985).
[30] In particular, if $q_1 = 1$ in Eq. (2), Eq. (3) defines a direct correspondence between $|\Psi_{\mathrm{FQH}}(K_1, K_2)\rangle$ and $|\Psi^{\mathrm{lat}}_{\mathrm{FQH}}(K_1, K_2)\rangle$. In this paper, we always set $q_1 = 1$ by choosing appropriate N_1 and N_2.
[31] A. M. Läuchli, E. J. Bergholtz, J. Suorsa, and M. Haque, Phys. Rev. Lett. **104**, 156404 (2010).
[32] Z. Liu, E. J. Bergholtz, H. Fan, and A. M. Läuchli, Phys. Rev. B **85**, 045119 (2012).
[33] E. J. Bergholtz and A. Karlhede, Phys. Rev. B **77**, 155308 (2008).
[34] M. P. Zaletel and R. S. K. Mong, Phys. Rev. B **86**, 245305 (2012).
[35] R. Thomale, A. Sterdyniak, N. Regnault, and B. A. Bernevig, Phys. Rev. Lett. **104**, 180502 (2010).
[36] E. J. Bergholtz, M. Nakamura, and J. Suorsa, Phys. E (Amsterdam) **43**, 755 (2011).
[37] E. H. Rezayi and F. D. M. Haldane, Phys. Rev. Lett. **84**, 4685 (2000).
[38] E. J. Bergholtz, J. Kailasvuori, E. Wikberg, T. H. Hansson, and A. Karlhede, Phys. Rev. B **74**, 081308(R) (2006); A. Seidel and D.-H. Lee, Phys. Rev. Lett. **97**, 056804 (2006).
[39] Y.-H. Wu, J. K. Jain, and K. Sun, Phys. Rev. B **86**, 165129 (2012).
[40] A. G. Grushin, T. Neupert, C. Chamon, and C. Mudry, Phys. Rev. B **86**, 205125 (2012).
[41] In the Wannier basis, this amounts to adding $\sum_{ij=0}^{N_1 N_2 - 1} \delta^{\mathrm{mod} N_2}_{i,j} \varepsilon_{ij} c_i^\dagger c_j$ with $\varepsilon_{ij} = \frac{1}{2}\sum_k (V^{\mathrm{FCI}}_{ikjk} - V^{\mathrm{FCI}}_{ikkj} - V^{\mathrm{FCI}}_{kijk} + V^{\mathrm{FCI}}_{kikj})$.
[42] X.-L. Qi, H. Katsura, and A. W. W. Ludwig, Phys. Rev. Lett. **108**, 196402 (2012).
[43] A. Chandran, M. Hermanns, N. Regnault, and B. A. Bernevig, Phys. Rev. B **84**, 205136 (2011).
[44] V. Alba, M. Haque, and A. M. Läuchli, Phys. Rev. Lett. **108**, 227201 (2012).
[45] Z. Liu, E. J. Bergholtz, H. Fan, and A. M. Läuchli, Phys. Rev. Lett. **109**, 186805 (2012).
[46] A. Sterdyniak, C. Repellin, B. A. Bernevig, and N. Regnault, arXiv:1207.6385.
[47] M. Barkeshli and X.-L. Qi, Phys. Rev. X **2**, 031013 (2012).
[48] C. H. Lee, R. Thomale, and X.-L. Qi, arXiv:1207.5587.